Final Report

On-board Diagnostic Sensor for Respirator Breakthrough

NIH Contract 1 R43 OH04174-01
SBIR Phase I

SUBMITTED BY

NANOMATERIALS RESEARCH

2021 Miller Drive
Longmont, CO 80501

Principal Investigator: B.K. Miremadi, D.J. Deininger

Co-investigators: E.J. Benstock, S.A. Hooker, C.J. Kostelecky, and S.S. Williams

Tel: (720) 494-8401 •Fax: (720) 494-8402

8/31/01

TABLE OF CONTENTS

1. LIST OF ABBREVIATIONS

Polyaniline (PANI)
Polypyrrole (PPY)
Polythiophene (PTh)
Tin oxide (SnO_2)
Oxygen (O_2)
Carbon Dioxide (CO_2)
Tetrahydrofuran (THF)
Methylethylketone (MEK)

2. LIST OF FIGURES

3. LIST OF TABLES

4. ABSTRACT

Nanomaterials Research has demonstrated the feasibility of developing an extremely sensitive, low temperature, low cost, and miniaturized chemiresistive sensor that can be mounted inside a respirator to warn users when toxic organic vapors are present inside the respirator. This sensor can alert the wearer when the respirator's filter cartridge is defective, when the respirator does not fit properly, or when the respirator has been compromised for any other reason. Current methods of predicting filter breakthrough are inexact and inefficient, so the development of a real-time, quantitative respirator sensor is an important achievement.

The Nanomaterials Research VOC sensor is based upon novel materials selection (including polymers and nano-scale ceramic powders) which overcomes present limitations of solid state sensor technology including: high operating temperature (300-400°C), significant power consumption (a result of the high operating temperature) and poor reproducibility from one sensor to the next. The development of new and unique polymer and ceramic composite materials for sensors has resulted in a sensor that is responsive to a wide range of toxic organic gases. If developed into a product, this sensor technology can result in dramatically increased levels of worker protection as well as significant cost savings because filter cartridges can be used more efficiently.

During the Phase I feasibility study, prototype nano-composite sensors were prepared and packaged using a commercial electronics package. These sensors were fully characterized for their response to a variety of VOCs including toluene, propanol, tetrahydrofuran (THF) and methylethylketone (MEK). The sensors were tested under a variety of conditions, including varying humidity, oxygen and carbon dioxide levels. The sensor response was excellent throughout the testing. Planned improvements in fabrication and packaging will lead to a low-cost, reliable sensor that is capable of operating on approximately 30mW of power.

5. SIGNIFICANT FINDINGS

1. High-quality sensors can be prepared using composite materials of nanostructured SnO_2 and conducting polymers. These sensors were demonstrated to respond to a variety of VOCs, including toluene, propanol, tetrahydrofuran (THF) and methyl ethyl ketone (MEK).
2. The detection limit of these sensors was more than adequate for the proposed application
3. The power consumption was approximately 100mW for the un-optimized sensors. Planned improvements can reduce this to 30mW.
4. The sensors respond well in the presence of humidity and are unaffected by changes in the level of oxygen and carbon dioxide present.
5. The sensor baseline and response is extremely stable over the course of a typical 8 hour workday.

6. USEFULNESS OF FINDINGS

The findings listed above are sufficient to demonstrate the feasibility of developing a sensor that can be mounted onboard a respirator. This sensor will then serve to warn the respirator wearer when vapors are entering the respirator for any reason, including a saturated cartridge or an ill-fitting respirator. A number of major respirator manufacturers have expressed interest in this technology.

7. SCIENTIFIC REPORT

7.1 SIGNIFICANCE OF THE PROBLEM

Air purifying respirators are worn when workers need to be protected from hazardous gaseous environments and the level of the toxic gas in the surrounding environment is less than the IDLH (immediately dangerous to life and health) limit. Respirators used in the above application utilize filters that are typically designed for specific classes of vapors such as acid gases or organic vapors.

Currently, the determination of when to replace filter cartridges during respirator usage is based upon a variety of factors. For cartridges that do not have an end of service life indicator (ESLI), the following methods are used.[1]

Manufacturers Objective Data: Test data may be available from the manufacturer of the respirator cartridge regarding the life expectancy of the cartridge. This method has some inherent risks associated with it in that it does not take into account specific operating conditions such as varying flow rates and humidity or the presence of other gases that might reduce the life expectancy of the cartridge.

Experimental Methods: Laboratory testing of experimental breakthrough time data may be obtained under worst case conditions. While this method is very safe and may provide more accurate data than some other methods, the testing is expensive and time consuming. Additionally, to the extent that the actual usage conditions are more benign than those of the test, the total capacity of the cartridge will not be used.

Mathematical Predictive Modeling: Mathematical modeling of life expectancy based on predictive equations is currently being developed. While the results of these methods are valuable, they are highly complex and require significant expertise and manufacturer's proprietary data. Additionally,

predictive models do not address changing concentrations and environmental conditions such as heat and humidity that might shorten the life of filter cartridges.

Analogous Chemical Structures: In some cases, employers can rely on breakthrough data and change out schedules based on other chemicals that are similar to the chemical of interest. In this case, the reasonable assumption is that a higher molecular weight substance would breakthrough no more rapidly than a lighter substance. While this is a reasonable assumption, it again does not take into account workplace-specific conditions and is likely to result in more frequent cartridge change out than is actually necessary.

Worker safety would certainly be improved by incorporating sensors directly into respirators to warn the wearer if toxic organic vapors had broken through the filter or if the filter or respirator had been damaged or dislodged. This technology would also provide significant cost savings to respirator users if the full capacity of the filter cartridges could be used.

Sensor Background

Chemiresistive sensors based on ceramic materials such as tin oxide are well known, both in the literature and in commercial practice. In general, most semiconductor metal oxides undergo surface interactions (physisorption and chemisorption) with gas molecules at elevated temperatures (300 to 600°C). Since most semiconductor sensors are polycrystalline (composed of multiple crystallite grains pressed or sintered into a continuous structure incorporating grain boundaries), the adsorbed gases have significant electronic effects on the individual crystalline particles. These gas-solid interactions, result in a change in electron (or hole) density at the surface (i.e., a space charge forms), which in turn results in a change in overall conductivity of the semiconductor oxide. An example of this is the interaction of SnO_2 or TiO_2 with molecular oxygen. O_2 chemisorbs on these materials, producing negatively charged oxygen ions, O^- and O_2^-, via removal of electrons from the conduction band of the metal oxide. Thus, there are fewer electrons in the surface space-charge region, and the overall conduction of the material is reduced. In the band gap model, the loss of electrons from the conduction band raises the conduction band energy, and thus widens the band gap. A similar interaction reaction occurs when reducing gases, such as H_2, interact with semiconductor surfaces, resulting in adsorbed positive ions, H_2^+ on the surface, and consequent donation of electrons to the conduction band, with a corresponding reduction in the band gap. In both cases, the nature of the interaction is ionic, and the presence of a gas changes the electronegativity of the metal oxide and the width of their band gaps. The accumulation of negative charges in n-type semiconductor oxides such as SnO_2 creates a narrowing of the band gap and an increase in conductivity, while a depletion of negative charges widens the band gap and thus results in a decrease in conductivity.

The sensors developed in Phase I are based upon the operating principle described above, with several innovative aspects:

- ***Creating "Nanocomposites"*** – The formation of a composite material containing both an organic polymer and a nanometer-scale metal oxide semiconductor is a key innovation enabling improved sensor performance. Through selection of the proper polymer, it is possible to selectively adsorb vapors of interest based on the relative solubility of the vapors in the polymer, while lowering the temperature at which these gas-surface interactions occur. When the grain size of the ceramic is on the nano-scale, we refer to these composites as "nanocomposites". The nanocomposite advantage is believed to be due to the selective partitioning of the gas of interest into the polymer – ceramic matrix

where it readily interacts with the ceramic material. The electrochemical properties of the composite will be altered by the presence of the dissolved vapor, allowing detection of the vapor via resistance measurements across the composite. The use of a polymer composite provides a matrix of uniformly distributed particles such that individual particles are contributing to the conduction as compared to a "chunk" of particles. Carefully selected conductive polymer materials such as polyaniline can also act as promoters by providing more electrically interconnected grain boundaries.

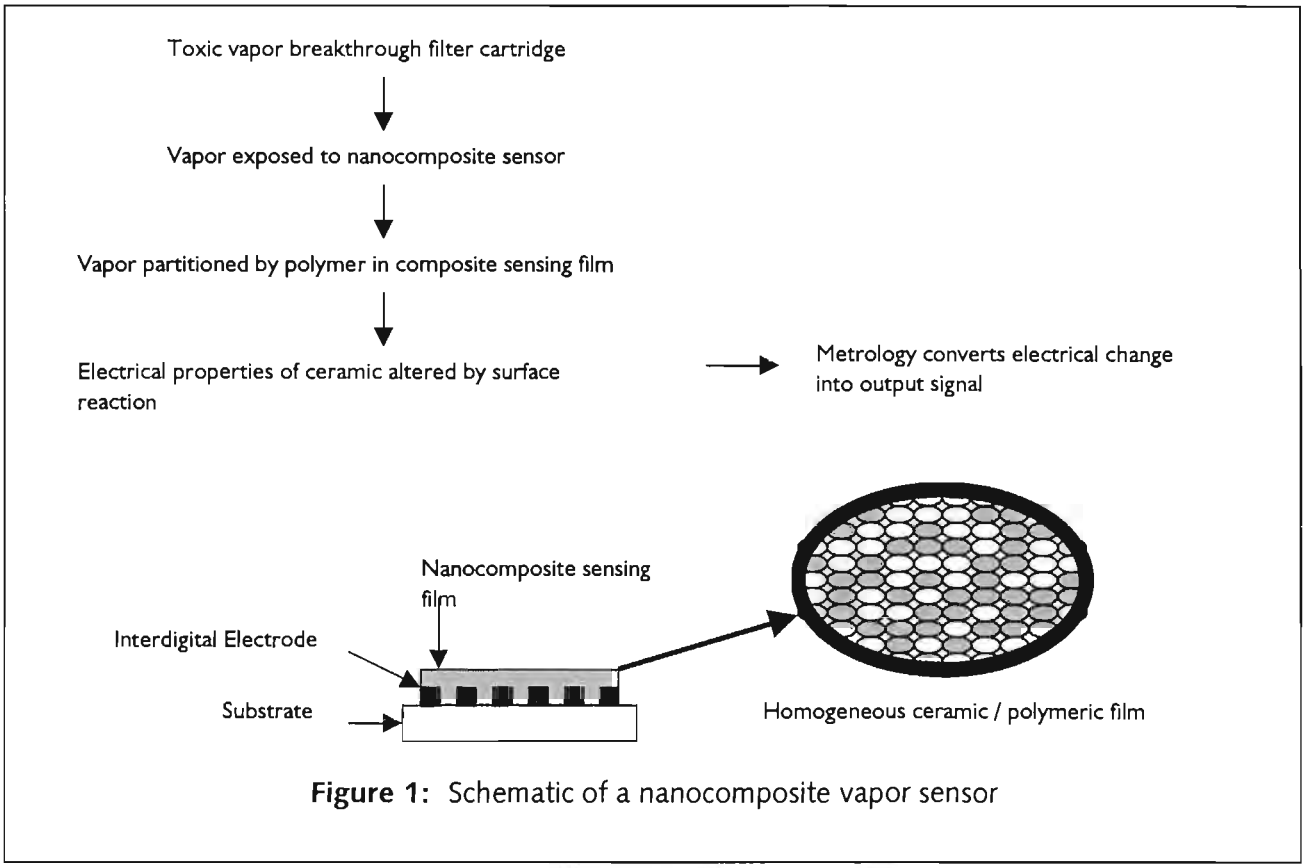

Figure 1: Schematic of a nanocomposite vapor sensor

- ***Introduction of Catalysts*** – Catalysts are used in conjunction with conventional solid-state sensors to promote a response to a particular gas (thereby improving sensitivity and selectivity). For example, noble-metal catalysts are often used to detect non-polar organics because they form strong homopolar or ligand field bonds with the adsorbate [2]. It should be noted that it is very important that the catalyst material be well dispersed over the semiconductor surface to ensure good performance. Nanomaterials Research has used a proprietary process that starts with colloidal materials that are easily distributed into the fine-grained ceramic matrix for maximum effect.
- ***Reducing Grain Size*** – Recently, several researchers [3,4,5,6] have reported a substantial performance increase in semiconducting metal oxide sensors as grain size is reduced to the "nano-scale" level. Perhaps the simplest explanation for this phenomenon rests in the fact that chemisorption (i.e., the underlying principle of these sensors) is primarily a surface effect. Chemisorbed oxygen ions act as surface acceptors, trapping electrons and forming a space charge layer. For example, in the case of SnO_2 in the presence of CO, these ions react to form CO_2, which vaporizes leading to a measurable conductivity change. To maximize the opportunities for such reactions to occur, a high ratio of surface area to

volume is needed. An inverse relationship exists between surface area and particle size; hence, ultra-fine-grained materials that offer very high surface area are desirable.

From a more theoretical perspective, one must consider the possible conduction mechanisms in semiconducting oxides. In polycrystalline materials, grain boundaries typically contribute most of the resistance, and conduction is controlled by an energy barrier established at the grain boundary due to the conduction band bending into the space charge layer. However, electrical conduction due to "necking" of individual grains is also possible. In this case, the material's resistance is modulated by the width of the bulk conduction channel, which narrows as the space charge layer forms. For large grains, the particle radius is much greater than the width of the space charge layer, prohibiting modulation. Consequently, both mechanisms contribute only when the individual grains are very small, thereby increasing response.

Furthermore, for sensor materials, it has been proposed that intra-grain resistance dominates when the individual grain size is less than twice the Debye length (a function of the space charge layer thickness). For sputtered films of SnO_2, this length has been determined to be 3 nm by Hall effect measurements [7]. Therefore, one can postulate that reducing the size of the sensing material to less than 100 nm increases response, and further reductions to the sub-10-nm regime can have a substantial effect on performance. In Phase I, we used "nanopowders" of the materials of interest, making use of the high surface area and fine particle size. Further reductions in size may be considered in Phase II.

7.2 PHASE I OBJECTIVES

The Phase I work plan listed the following major objectives:

1. Fabrication and preliminary evaluation of nanocomposite sensing elements.
2. Characterization of the best nanocomposite sensing elements for the target application.
3. Preliminary sensor development, including package design, circuitry and cost estimates.
4. Evaluation of application requirements in preparation for Phase II.

7.3 PHASE I RESULTS

7.3.1 Preparation of Sensing Elements

A screen printing process was used to prepare sensing elements. New sensing materials were evaluated by preparing films of the sensing materials on ¼ inch substrates, which were then tested in our heated test block. The substrate used to prepare the sensors was a three inch square alumina substrate laser scribed into ¼ inch sections. An interdigitated gold electrode array was printed and fired using a commercial paste. Next, a proprietary sensor paste was prepared by combining a nanostructured semiconductor material with polymers and

Figure 2: ¼" by ¼" sensing element

catalysts in a commercial vehicle. This paste was thoroughly mixed using a three roll mill, then screen printed to provide a uniform layer of sensing material on top of the electrodes. The resulting sensor elements were thermally cured at a temperature below the glass transition temperature of the polymer to form a robust sensor film, as shown in Figure 2.

Packaged Sensors

A few of the best sensor compositions were tested more extensively as packaged sensors. In this case, the sensors were self-heated instead of being heated externally as was done with the preliminary screening experiments.

To prepare the packaged sensors, a resistive heater material with electrical contacts was screened onto the substrates prior to the active sensor paste. The screening process consisted of the following layers.

1. Electrical contacts for heater printed with a commercial gold paste.
2. Heater element printed with a commercial resistive paste of ruthenium oxide/palladium.
3. Dielectric layer printed to electrically insulate the heater from the sensor element, using a commercial paste.
4. Interdigitated array for electrical contact to the active sensor element printed using commercial gold paste.
5. Active sensor material printed from Nanomaterials Research proprietary paste.

The resulting sensor elements were then packaged into a commercially available TO-39 header using silver wire and conductive epoxy to make the electrical connections from the sensor element to the package pins. Two of these sensors are shown in Figure 3. A metal cap with a screen-covered opening was then glued onto the header using super-glue to protect the sensor elements during handling and testing. The sensors are heated by applying a constant voltage to the heater. Calibration curves have been prepared that relate the variables of voltage, power consumption and element temperature. Element temperature was measured using both a thermocouple and an IR thermometer. The elements are operated by providing either a constant or varying input voltage to the heater, while measuring the resistance of the sensor material.

Figure 3: Sensor elements packaged in commercial headers

A variety of polymer and ceramic materials were screened and tested as composite sensors in order to study the effect of sensor composition on response and resistance as a function of temperature. Table 1 is a list of polymers that were evaluated during the early months of this project., along with glass transition temperature (T_g) and melting temperature (T_m) where available [8,9]. In many cases, the T_g and T_m are not available. All of the polymers used in this project were bought as powders from commercial suppliers.

The semiconductors tin oxide (SnO_2), zinc oxide (ZnO), and iron oxide (Fe_2O_3) were studied in combination with the polymers listed above. All three of these semiconductors have been reported to show responsiveness as gas sensors. By far, the best response was seen with the SnO_2 composite sensors. In part, this was due to the lower resistance of these films in air, as well as the higher sensitivity to the challenge gases. The Fe_2O_3 films, in particular, had resistances greater than 100MΩ at all conditions, and the resistance of the sensor elements was too high to be measured using our equipment at many of the test conditions (i.e. >300MΩ).

Table 1: Polymers evaluated for suitability as composite gas sensors

Polymer:	T_g (°C)	T_m (°C)
Polyaniline		>320
Polypyrrole		
Polythiophene		> 350
Poly(vinyl chloride)	~85	
Polysulfone	183	
Polystyrene	100	

7.3.2 Characterization of Sensing Elements

For each composition studied, ¼" sensor elements were prepared as described above and tested using our custom heated test block. The test block was used to control the temperature of sensor elements under test at temperatures ranging from 50°C to 250°C. Challenge gas mixtures were blended using MKS mass flow controllers, and resistance data was acquired using a Keithly multiplexer and a Quadtech LCR meter. Temperature, gas flow, and data acquisition were all computer controlled using custom Labview programming created in house.

Thirty-one unique sensor compositions were screened for their response to the four target VOCs (toluene, propanol, methyl ethyl ketone and tetrahydrofuran) at temperatures ranging from 50°C to 250°C. The upper temperature limit was limited by the T_m and/or T_g of the polymer used. Based on these preliminary screening tests, several compositions were selected for further study. One composition was a doped SnO_2, two were composites of SnO_2 and polyaniline, while the third composition was a composite of SnO_2 and polythiophene. Table 2 summarizes the response of these compositions to the four target challenge gases. The response is calculated as the resistance of the sensor in air divided by the resistance in challenge gas (R_a/R_g). The polythiophene and polyaniline composites were tested with 200 ppm of each challenge gas at 250°C. The doped SnO_2 sensors were tested at 300°C with 500 ppm of each challenge gas.

Table 2: Comparison of best sensor element compositions

	propanol	toluene	MEK	THF
1% PTH + SnO_2, dry	461	138	71	379
1% PTH+ SnO_2, humid	109	45	39	45
5% PANI + SnO_2, dry	158	103	254	155
5% PANI + SnO_2, humid	24	14	39	55
10% PANI + SnO_2, dry	28	21	84	80
10% PANI + SnO_2, humid	20	10	35	41
Doped SnO_2, dry	1246	743	661	10,710

Each of these compositions showed an excellent response in both dry and humidified gas streams. Additionally, the response and recovery times are faster for the humidified sample stream. Unfortunately, there is a significant variation in sensitivity on switching from a dry to a humidified sample stream. This is not anticipated to cause a significant problem because further studies have

shown that the sensors are relatively unaffected by changing humidity levels, only the switch from very dry (cylinder) gases to a humidified sample stream. In the intended application, some humidity will always be present.

Humidity Barrier Coatings

Although these sensors are remarkably stable in the presence of varying amounts of water vapor (10-90% relative humidity) there is an unfortunate decrease in resistance on switching from dry gas to humid gas. This is primarily a problem in that it makes calibration slightly more difficult, because calibration gases should be humidified prior to calibrating the sensor.

Several coatings were tested in an effort to create a more hydrophobic sensor surface and hence eliminate the response of these sensors to humidity. The barriers tested included silicone spray, Teflon spray, Teflon dispersion and Nanomaterials Research's proprietary salt formulation, which has successfully reduced the humidity response of other sensor compositions. All of the coatings caused a significant decrease in the response of the sensors in both dry and humid gases. In the respirator application that this project has focussed on, a significant amount of water vapor will always be present, so the barrier coating studies were dropped after the early failures.

7.3.3 Packaged Sensor Elements

Several of the best sensor compositions were packaged into commercial headers as described earlier and were extensively characterized as packaged sensors using our prototype test system. This test system consists of a full set of MKS flow controllers, with a BK Precision Technologies power supply, custom circuitry and a computer controlled data acquisition system featuring National Instruments DAQ cards and Labview software. There are several advantages to carrying out characterization testing on packaged sensors. First, the sensors are self-heated using a resistive heater which is printed beneath the active sensor material, which is the same way the sensors will be heated during use. Second, by virtue of its design, this test system is capable of testing sensors with higher resistance values and it records data significantly faster which leads to more accurate response time measurements.

The sections below summarize the responses of sensors when tested under variety of operating conditions and gas exposures.

Operating Temperature

Sensor AB095-01 (modified SnO_2)

This sensor responds well at temperatures as low as 150°C, although a temperature of 200°C was chosen for the testing because of its higher sensitivity. Figure 4 shows the response of this sensor to 200 ppm toluene at temperatures ranging from approximately

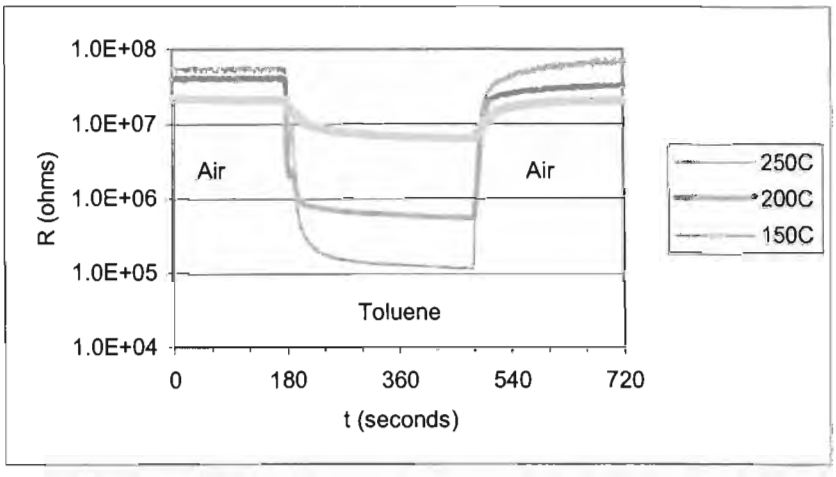

Figure 4: Response of composition AB095-01 to 200 ppm toluene.

150 to 250°C. In this series of experiments, the sensors were exposed to an atmosphere of background air for a period of 180 seconds, followed by an exposure to 200 ppm toluene for 300 seconds, then a return to air. Throughout the experiment, the challenge gas was humidified to a level of approximately 40% RH in order to better simulate the intended application of respirator usage.

For this type of sensor, the response is frequently calculated by dividing the resistance of the sensor in air by the resistance of the sensor in challenge gas. By this definition, the response at 200°C was 96, which is an excellent response. By comparison, the response at 150°C was only 3.3.

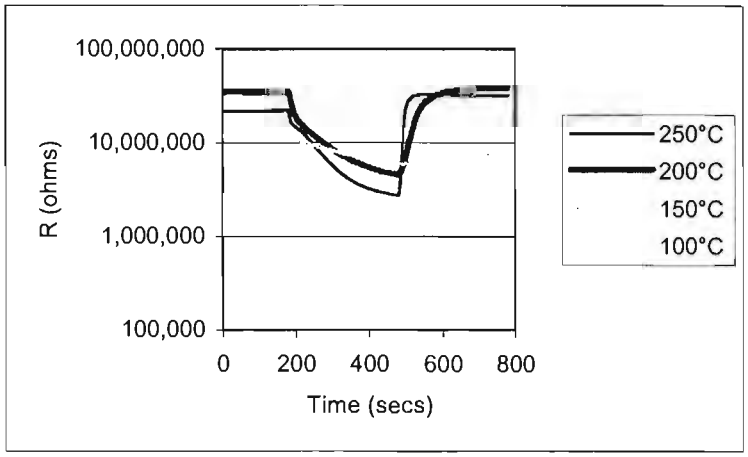

Figure 5: Response of composition AB095-02 to 200 ppm toluene

AB095-02 (SnO_2/ PANI/ catalyst)

This sensor responds very well at temperatures of 200°C and 250°C as shown in Figure 5. As before, the sensor was held in air for 180 seconds, then the challenge gas of 200 ppm toluene was applied for 300 seconds, and then the sensor was returned to an air atmosphere. All gas samples were humidified to approximately 40% RH. The sensor response at 150°C is significantly smaller than the response at higher temperatures, while the response at 100°C is nearly non-existent. The response at 200°C was by far the largest for this composition, therefore subsequent testing focused on this temperature.

Table 3 provides a comparison of the two preferred sensor compositions at the temperatures tested. In each case, the challenge gas was 200 ppm toluene.

Table 3: Comparison of sensitivity (Rair/Rgas) at temperature for two sensor compositions.

	250°C	200°C	150°C	100°C
AB095-01	326	96	3	
AB095-02	7	9	2	1

Linearity/Selectivity

The linearity and selectivity of the each of the sensor compositions was studied at the target temperature. The organic gases propanol, toluene, tetrahydrofuran and methyl ethyl ketone were tested at concentrations ranging from 50 ppm to 500 ppm. Additionally, carbon dioxide (CO_2) was tested at levels ranging from 350 to 5000 ppm. Carbon dioxide is an important interferant gas to study for this application, as it is likely to be present at significant concentrations in a stream of exhaled breath.

AB095-01

The response of the modified SnO_2 sensors to all of the challenge gases and to background air is shown in Figure 6. Each gas was tested at the concentrations listed in the presence of approximately 40% relative humidity. The varying concentrations were tested in a random order and the 250 ppm concentration of each gas was tested first and last to ensure that there were no hysteresis effects during gas testing.

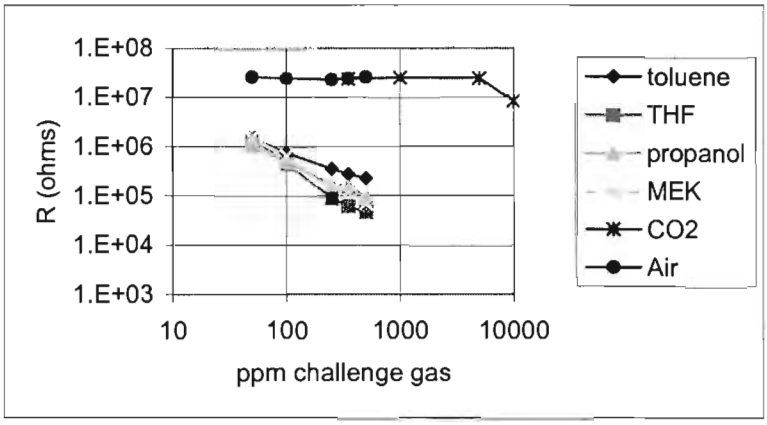

Figure 6: Selectivity and Linearity of AB095-01

This sensor is very sensitive to the four organic gases, with a similar response to each gas. The response is approximately linear when viewed on a log-log scale. The sensors do show a very small response to CO_2; however, this response is insignificant compared to the magnitude of the sensor response to the target gases.

AB095-02

The response of the SnO_2/PANI sensors was tested in the same manner as the modified SnO_2 sensors, and the results are shown in Figure 7. As compared to the modified SnO_2 sensors, the SnO_2/PANI composition is more sensitive to some of the VOC challenge gases (THF and MEK) and less sensitive to others (toluene and propanol). The sensor composition is also slightly more sensitive to CO_2. Thus, in a comparison of selectivity and linearity, neither sensor composition has a clear advantage over the other.

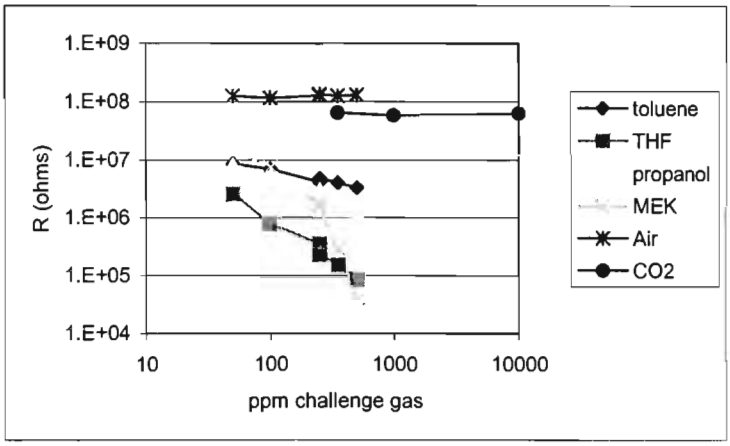

Figure 7: Selectivity and Linearity of AB095-02

Humidity

All of the characterization tests have been carried out in the presence of a small amount of water vapor, because the atmosphere inside a respirator is likely to contain water vapor. For the purposes of the sensor characterization, all of the tests have been carried out in the presence of approximately 40% relative humidity.

In this particular test, the response of the sensor to changing relative humidity levels from 0% (dry cylinder air) to ~85% was tested, and the results are shown in Table 4. The relative response of each sensor composition to humidity was determined by comparing the response at 42% RH to the

response at each humidity level. This is analogous to the response calculation used for the target gases.

Table 4: Response of the sensor to changing humidity levels

Relative Humidity	AB-095-01 Resistance kΩ	AB-095-01 Relative Resistance R (42% RH)/R (x%RH)	AB-095-02 Resistance kΩ	AB-095-02 Relative Response R (42% RH)/R (x%RH)
0% RH	5,286	1.85	298,000	0.25
21% RH	9,883	0.98	95,000	0.77
42% RH	9,565	1.00	73,000	1.00
63% RH	14,217	0.66	72,000	1.02
85% RH	14,783	0.64	46,000	1.61

The data show a small change in resistance with changing humidity levels, which is insignificant compared to the response of the sensor to challenge gas, which is approximately 90 at 200 ppm. Additionally, the largest error is seen in the transition from dry air to humid air, which is not an issue in this application, where some humidity will always be present.

Flow Rate Response

One group of sensors was tested at flow rates ranging from 100 ml/min to 1000 ml/min and the results are shown in Table 5. The challenge gas in this test was 200 ppm toluene. As expected, the sensors showed a variation in response with flow rate.

Table 5: Flow rate response of AB095-01

Flow rate	Sensitivity (Ra/Rg)
100 ml/min	72
250 ml/min	756
500 ml/min	830
750 ml/min	448
1000 ml/min	229

Typically sensors of this type do show a response to changing flow rates, because the flow rate is directly related to how much gas reaches the surface of the sensor. Additionally, very high flow rates can reduce the response of the sensor by cooling the sensor surface. These effects are seen in Table 5, where the response of the sensors is a function of flow rate, especially at very high and very low flow rates. At very low flow rates, the sensor response is reduced because there is less challenge gas reaching the surface of the sensor. At very high flow rates, the sensor response is reduced due to cooling effects. This sensor behavior is typically handled through the design of the sensor packaging. The final package design will be done in such a way as to minimize or eliminate these effects.

Oxygen Effects

The oxygen level testing, shown in Figure 8, showed that the sensors are not particularly dependent on the amount of oxygen present. Each sensor response is the average of 4 sensors. Although the response of these sensors requires the presence of some oxygen on the surface of the sensor, variations in the amount of oxygen over the range of 16-22% do not affect the response of the sensor. This is important for the intended application, where oxygen levels can fluctuate with changes in barometric pressure and exhalation of the subject wearing a respirator.

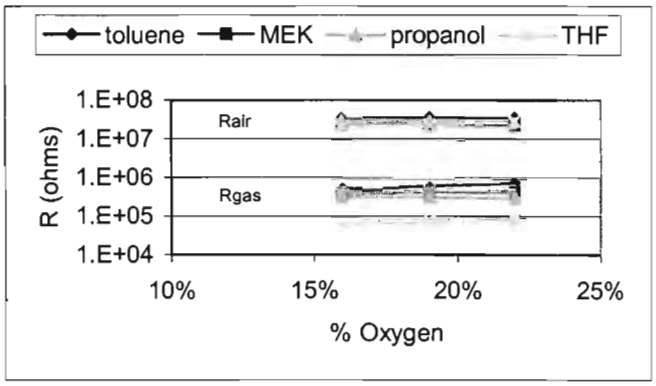

Figure 8: Variation in response of AB095-01 with oxygen level

Response Time:

The response time for the two best compositions was calculated as the time to reach 90% of the full response (t_{90}), and is shown in Table 6. The 90% response was calculated as shown in equation 1.

$$R(90\%) = Rair - 0.9(Rair - Rgas) \quad (1)$$

The response time was calculated for two different gas concentrations, as our experience has shown that the response of the sensors is often faster at higher concentrations. This result is shown in the data below. In all cases, the response time of these sensors was extremely fast, and is more than adequate for the intended application.

Table 6: Response time (t_{90}) of two sensor compositions

	AB095-01		AB095-02	
Challenge Gas	50 ppm	500 ppm	50 ppm	500 ppm
MEK	5 s	2 s	6 s	3 s
Propanol	4 s	2 s	4 s	2 s
THF	4 s	2 s	21 s	18 s
Toluene	7 s	3 s	4 s	4 s

Stability

Both short and long-term stability of the sensors was evaluated, although the length of the long-term stability testing was necessarily limited by the constraints of the Phase I work period. Table 7 shows the short-term stability of the baseline resistance of the sensors. At 4 hours, all of the baseline resistances were within 2% of the resistance value recorded at 1 hour. At 8 hours, all of the baseline resistances were within 3% of the initial value and 6 out of 8 of the sensors were still within 2% of the initial value. These are very good results for workday stability, which show that

the sensors may be operated continuously during a single shift without the need to worry about calibration or baseline reset issues.

Table 7: Variation in baseline of AB095-02 sensor compositions

Time	Sensor #							
(hours)	1	2	3	4	5	6	7	8
1	100%	100%	100%	100%	100%	100%	100%	100%
4	98%	100%	99%	102%	99%	99%	98%	102%
8	101%	102%	99%	103%	99%	99%	97%	103%

The longer term stability of the sensors was also evaluated. Figure 9 and Figure 10 show the response of 5 typical sensors. The sensors were exposed to a low (100 ml/min) flow rate of 200 ppm propanol as shown in Figure 9. In this experiment, the sensors were exposed to a sequence of air, 200 ppm propanol, air, 200 ppm propanol and air for 180 seconds each. All challenge gases were humidified to approximately 42% RH by passing part of the air sample stream through a bubbler of deionized water. Next, the test system was set to record a data point every 5 minutes for a period of 3 ½ days while the sensors were exposed to a constant stream of humidified air. The flow of the humidified air stream was set at a flow rate of 100 ml/min. The results of this test are shown in Figure 10.

After the first four hours of stabilization time, the average drift in sensor was 9%, which is less than the 10% called for in the feasibility criteria of the Phase I proposal. Additionally, it is well known that chemiresistive sensors typically take several weeks to stabilize completely at temperature. For example, Figaro (the leading supplier of tin oxide chemiresistor sensors) recommends a minimum 7 day pre-heating prior to sensor testing.[10] Unfortunately, the luxury of long stabilization times was not available due to the time constraints of the Phase I project. Thus, the stability of the sensors can reasonably be expected to improve with continued testing.

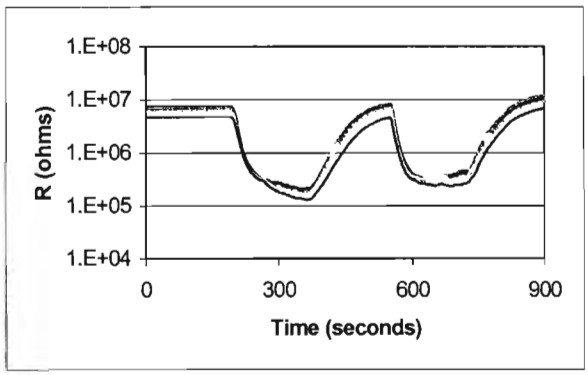

Figure 9: Response of 5 typical composite sensors to 200 ppm propanol

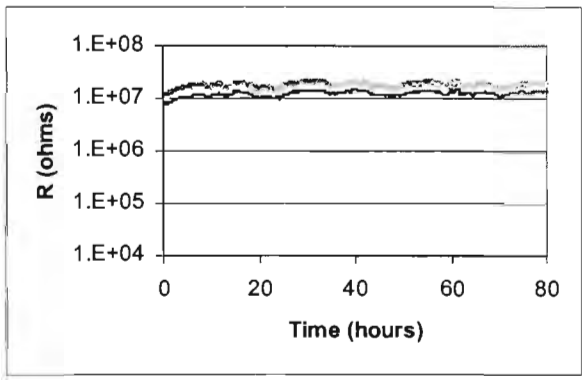

Figure 10: Resistance of 5 typical composite sensors held in a humidified air stream.

Detection Limits:

During the Phase I effort, the sensors were tested at concentrations ranging from 50 to 500 ppm, which is an appropriate range for the gases of interest. Table 1 shows the NIOSH STEL and TWA limits for the gases studied during the Phase I.

For each sensor composition, an estimate of the detection limit for each of the gases was also calculated through extrapolation of the data. Because the sensors respond in a logarithmic fashion to gas, a log-log plot of resistance versus concentration was prepared and a linear curve fit applied. The linear curve fit was then used to calculate the concentration of gas required to cause a change in resistance greater than three times the noise in the baseline resistance.

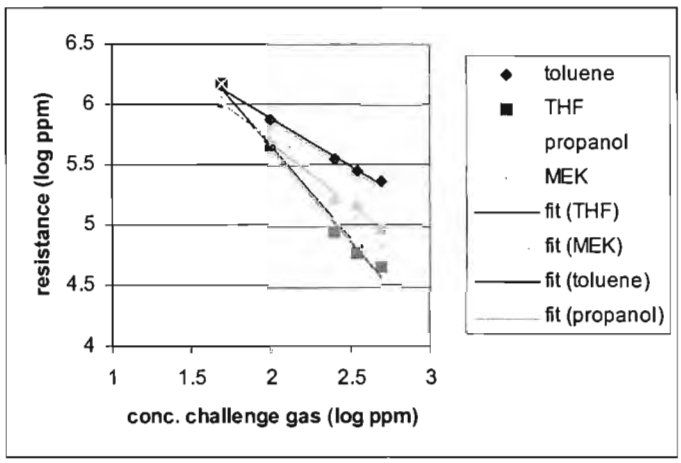

Figure 11: Linear curve fit to log-log plot of resistance versus concentration for AB095-01

Figure 11 shows the linear curve fit on the log-log plot of resistance versus concentration for sensors AB095-01. A similar plot was prepared for sensor composition AB095-02. From the calculations described above, an estimate of the concentration required to give a signal of three times the noise level was calculated for each gas. These results are shown in Table 9.

Table 8: NIOSH STEL and TWA limits for selected gases

Challenge Gas	NIOSH STEL (ppm)	NIOSH TWA (ppm)
1-propanol	250	200
Toluene	150	100
THF	250	200
MEK	300	200

Cyclic Studies

Although the composite sensors developed during this Phase I effort operate at relatively low temperatures, it is nonetheless evident that in order to develop a battery powered device, the power consumption of the sensors must be further reduced. It is our opinion that in order to achieve the ultra-low power consumption required for this application, the sensors will need to be operated in a cyclic manner, whereby power is applied to the heater only a fraction of the time. We have therefore conducted some preliminary studies aimed at demonstrating the feasibility of operating the sensors in a pulsed mode. These efforts were very successful, and they lay the groundwork for further reduction of power consumption during Phase II through optimization of the temperature cycling methodology.

Table 9: Sensor element detection limits

Challenge gas	Estimated detection limit (ppm) AB095-01	AB095-02
Toluene	2	2
THF	9	8
1-Propanol	3	10
MEK	7	1

Figure 12 shows the response to 200-ppm challenge gas of a single sensor when operated at a variety of timing cycles. The sensor tested was a SnO_2/PANI composite previously identified as AB095-02. In this

case, during the time labeled as "hi" a voltage of 7.2V was applied to the resistive heater. This voltage was sufficient to heat the sensor element to 250°C during continuous heating. The low voltage was set at~.5 volt, and was sufficient to heat the sensor element to only 50°C on continuous operation.

Clearly, reducing the proportion of time with the heater on reduces the sensitivity and increases the response and recovery time of the sensors. This data shows that a reduction in operating voltage to a 50% duty cycle (3 seconds "hi", 3 seconds "lo") is readily achievable without a significant degradation in sensor performance. Additionally, a 33% duty cycle is also feasible, without too severely impacting the sensor performance. At a 33% duty cycle, however, the recovery time of the sensor is noticeably lengthened.

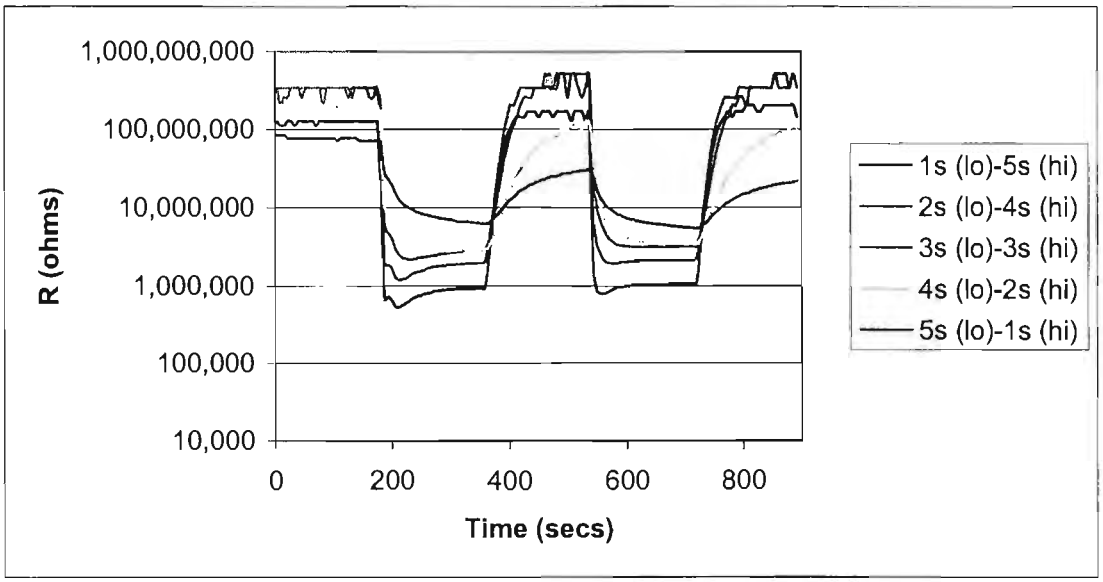

Figure 12: Response to 200 ppm propanol of temperature cycled composite sensor

7.3.4 Preliminary Design Concept for Integration into Respirator

Although the major goal and effort of the Phase I feasibility study was the development of the sensor technology, a secondary but important task was to develop a preliminary design concept for the integration of this sensor into a respirator. The circuitry required to operate a sensor of this type is relatively straightforward, although the need for low power considerations does complicate things slightly.

Operating power and circuitry

The power input to heat and operate the sensor is a DC voltage input to an onboard resistive heater. Preliminary testing has been shown that power cycling will likely be required to minimize the power consumption of the sensor. Most likely, the power input will cycle between 2 voltages, or possibly an on/off configuration. As mentioned earlier, the minimization of power required for sensor operation will be a key requirement for the Phase II design effort. The sensor elements produced and packaged during the Phase I feasibility study were 1/8" (125 mil) square and

packaged in a commercial header, referred to as a TO-39 package. The power requirement for these elements operating at peak temperatures was approximately 500 mW. Planned improvements include reducing the size of the sensor to 75 mil by 75 mil, for a total reduction in area of 44%, which is not expected to reduce sensor performance. Additionally, the thickness of the substrate used to prepare the elements can be reduced from 10 mil to 8 mil, for a further reduction in mass of approximately 18%. Our calculations have shown that these simple improvements can lead to a reduction in peak power consumption from 500 mW to approximately 150 mW. During Phase I, we also conducted some preliminary experiments to examine the feasibility of temperature cycling as a means of power reduction. By operating the sensor element at peak power only 20% of the time (with essentially no power consumption during the remaining cycle) we have shown that we can further reduce the power consumption to approximately 30 mW. Furthermore, we believe that with optimization of the temperature cycling, we may be able to reduce the peak power to just 10% of the duty cycle, resulting in a target power consumption of the finished, packaged sensor of 15-30 mW. These numbers are low enough to allow operation of the monitoring sensor and circuitry using a Li ion coin cell type of battery. For example, using a 1000 mAh capacity coin cell (e.g. Panasonic part number CR 2477 or BR2477A/FB) will allow a battery lifetime of approximately 100 hours of operation time.

Production cost

We have also developed some very preliminary cost targets for the production of these sensors in order to demonstrate the financial feasibility of developing this type of product.

The sensor elements will be prepared via a screen printing process. As discussed earlier, this is a five step printing process. With a reduced element size of 0.075 by 0.075 inch, sensor elements can be printed in lots of 1600. Allowing time for set up, printing, and clean up, we have estimated a production cost of less than $0.10 per element. Further costs will obviously be incurred during testing and packaging of the sensors. These costs will be minimized via design for manufacture (DFM) techniques utilized during the Phase II effort. Because the final design will depend heavily upon input from industrial partners, it is difficult to accurately estimate the final cost of the packaged sensor at this time. A likely target cost will be <$2.00 (preferably $1.00) for sensor, package and circuitry.

A significant capital investment will be required to produce these sensor elements in volume. Likely acquisitions will include an automatic screen printer, element handling equipment, a custom test system and an injection mold for the packaged sensors. Circuit boards will be built by an outside supplier in order to keep costs low. Many manufacturers specialize in supplying circuit boards to instrument and device manufacturers.

7.3.5 Commercialization Potential

During the course of the Phase I project, the midpoint results were presented to a number of major respirator manufacturers at the American Industrial Hygienists Conference and Exposition (AIHCE) in New Orleans in June. There was considerable interest in this technology, and discussions are ongoing with several of the companies. Table 10 is a list of the respirator manufacturers who were contacted and showed interest in this technology at the AIHCE show.

Table 10: Respirator manufacturers contacted regarding this technology

Company	Location	Web Address
Scott Health and Safety	Monroe, NC	www.scotthealthsafety.com
Survivair	Santa Ana, CA	www.survivair.com
North	Cranston, RI	www.northsafety.com
The S.E.A. Group	Branfor CT	www.sea.com.au
3M Occupational Health and Env. Safety Div.	St. Paul, MN	www.3m.com/occsafety
Moldex	Culver City, CA	www.moldex.com
Dalloz Safety	Reading PA	www.dallozsafety.com
MSA	Pittsburgh, PA	www.MSAnet.com

7.4 PHASE I CONCLUSIONS AND OUTLOOK FOR PHASE II

The criteria listed below were identified in the Phase I proposal as essential for demonstration of feasibility. The following paragraphs detail our success at meeting these criteria.

1. Sensors are capable of consistently responding to challenges of a subset of the following gases: formaldehyde, 1-propanol, toluene, tetrahydrofuran, isopropyl acetate, MTBE, MEK, and hexane. The detection limit must be less than the NIOSH STEL limit, and should ideally be lower than the NIOSH TWA limit.

   The sensors were tested at concentrations as low as 50 ppm, which is lower than the NIOSH STEL and TWA limits. Additionally, the detection limits of the sensors was calculated for each challenge gas and are reported in Table 11 along with the regulatory exposure limits. Clearly, the detection limits are well below the limits required for NIOSH and are sufficient to provide an advance warning before the worker is any danger of exposure.

Table 11: Sensor response to target gas concentrations

Challenge Gas	NIOSH STEL (ppm)	NIOSH TWA (ppm)	Min. Conc. Tested (ppm)	Est. Detection Limit (ppm)
1-propanol	250	200	50	<10
Toluene	150	100	50	<5
THF	250	200	50	<10
MEK	300	200	50	<10

2. Sensors show baseline drift of <10% over the course of weeks, and 2% over the course of hours.

   As shown in Table 7, the variation in sensor baseline drift over a 4 hour period is 2% or less. Eight sensors were tested. A further test of 5 sensors showed an average variation in resistance of 9% over the course of several days, with the sensor stability increasing with time.

3. Sensor response to the target gases is not significantly diminished by exposure to high levels of relative humidity

All of the characterization tests were carried out in the presence of approximately 40% relative humidity. Additionally, the response of the sensor to changing humidity levels was characterized from 0% to 85% RH. The response of the sensor is very good at all humidity levels and the sensor is not significantly affected by changing levels of humidity. Table 4 shows the response of the sensors to changing humidity levels.

4. Power consumption of sensors is less than 250mW in a standard sensor package.

   The estimated power consumption of the sensor elements produced and tested via temperature cycling during Phase I was 100mW. These sensors were packaged in a commercially available TO-39 electronics package. Planned improvements have been suggested that can reduce the power consumption to 30 mW as discussed in the preceding section.

8. PUBLICATIONS

No publications have resulted from this work.

1 OSHA directive CPL 2-0.120 – "Inspection procedures for the Respiratory Protection Standard," Appendix A

2 M.J. Madou and S.R. Morrison, Chemical Sensing with Solid State Devices, New York: Academic Press, 1989.

3 ibid

4 Jin, Z., et al., "Application of Nano-Crystalline Porous Tin Oxide Thin Film for CO Sensing," *Sensors and Actuators B* **52** 188-94 (1998).

5 Varghese, et al., "High Ethanol Sensitivity in Sol-Gel Derived SnO_2 Thin Films," *Sensors and Actuators B* **55** 161-5 (1999).

6 Wu, N.L., Wang, S.Y., and Rusakova, I.A., "Inhibition of Crystallite Growth in the Sol-Gel Synthesis of Nanocrystalline Metal Oxides," *Science* **285** 137-9 (1999).

7 Varghese, et al., "High Ethanol Sensitivity in Sol-Gel Derived SnO_2 Thin Films," *Sensors and Actuators B* **55** 161-5 (1999).

8 Aldrich Chemical Catalog, Sigma-Aldrich Co.,2000-2001

9 J. Brandrup, E.H. Immergut, E.A. Grulke, Polymer Handbook, 4th ed., New York, John Wiley and Sons, Inc., 1999.

10 http://www.figarosensor.com/products/general.pdf

NANOMATERIALS

Equipment Inventory
NIH Contract 1 R43 OH04174-01
SBIR Phase I
Nanomaterials Research

No equipment was puchased during this project.

DEPARTMENT OF HEALTH AND HUMAN SERVICES

Public Health Service
Centers for Disease Control
and Prevention (CDC)

Memorandum

Date: March 28, 2002

From: Lee M. Sanderson, Ph.D., Program Official
Office of Extramural Programs, NIOSH, E-74

Subject: Final Report Submitted for Entry into NTIS for Grant 1 R43 OH004174-01.

To: William D. Bennett
Data Systems Team, Information Resources Branch, EID, NIOSH, P03/C18

The attached final report has been received from the principal investigator on the subject NIOSH grant. If this document is forwarded to the National Technical Information Service, please let us know when a document number is known so that we can inform anyone who inquires about this final report.

Any publications that are included with this report are highlighted on the list below.

Attachment
cc: Sherri Diana, EID, P03/C13

List of Publications

Title: On-Board Diagnostic Sensor for Respirator Breakthrough
Investigator: Bijan K. Miremadi, Ph.D.
Affiliation: Superior Sensing Solutions
City & State: Longmont, CO
Telephone: (303) 702-1672
Award Number: 1 R43 OH004174-01
Start & End Date: 9/30/2000–6/30/2001
Total Project Cost:
Program Area: Control Technology
Key Words:

Abstract:
Nanomaterials Research has demonstrated the feasibility of developing an extremely sensitive, low temperature, low cost, and miniaturized chemiresistive sensor that can be mounted inside a respirator to warn users when toxic organic vapors are present inside the respirator. This sensor can alert the wearer when the respirator's filter cartridge is defective, when the respirator does not fit properly, or when the respirator has been compromised for any other reason. Current methods of predicting filter breakthrough are inexact and inefficient, so the development of a real-time, quantitative respirator sensor is an important achievement.

The Nanomaterials Research VOC sensor is based upon novel materials selection (including polmers and nano-scale ceramic powders) which overcomes present limitations of solid state sensor technology including: high operating temperature (300-400C), significant power consumption (a result of the high operating temperature) and poor reproducibility from one sensor to the next. The development of new and unique polymer and ceramic composite materials for sensors has resulted in a sensor that is responsive to a wide range of toxic organic gases. If developed into a product, this sensor technology can result in dramatically increase levels of worker protection as well as significant cost savings because filter cartridges can be used more efficiently.

During the Phase I feasibility study, prototype nan-composite sensors were prepared and packaged using a commercial electronics package. These sensors ere fully characterized for their response to a variety of VOCs including toluene, propanol, tetrahydrofuran (THF) and methylethylketone (MEK). The sensors were tested under a variety of conditions, including varying humidity, oxygen and carbon dioxide levels. The sensor response was excellent throughout the testing. Planned improvements in fabrication and packaging will lead to a low-cost, reliable sensor that is capable of operating on approximately 30mW of power.

Publications
No publications to date.